JOURNAL OF APPLIED POLYMER SCIENCE VOL. 21, 1699–1713 (1977)

Effect of Spin Orientation on Drawing of Wet-Spun Fibers

D. R. PAUL* and A. L. McPETERS, *Monsanto Triangle Park Development Center, Inc., Research Triangle Park, North Carolina 27709*

Synopsis

A previous study has shown that the draw stress of wet-spun acrylic fibers is affected by the orientation acquired in the spin bath, and a tentative mathematical treatment was proposed which employs an analogy with two-stage drawing. In this picture, the spin bath orientation is characterized by an effective draw ratio $\mathcal{R}_s$, the orientation draw is characterized by $\mathcal{R}$, and the total draw ratio $\mathcal{R}_t$ equals $\mathcal{R}\mathcal{R}_s$. This concept is developed more extensively in this paper. New data are presented on both acrylic and modacrylic fibers which support the validity of this treatment and also demonstrate how spin orientation is correlated with the take-up speed/free velocity ratio. Absolute values for the effective spin orientation are calculated. Results from round spinneret holes and one-slot hole are discussed with observations on shape retention.

INTRODUCTION

Most fiber processes include a drawing operation which reduces the denier of the filaments and increases molecular orientation to yield desirable fiber tensile properties. More complete knowledge of drawing and its interaction with other process steps is essential for developing an adequate understanding of the overall spinning process and the properties of resulting fibers. In a previous paper concerned with the wet spinning of acrylic fibers,[1] the stress required to draw fibers was used as an experimental tool to study the drawing step. In that paper, it was shown that draw stress was affected by the kinematics or rheology of fiber formation, presumably owing to orientation acquired in the spin bath prior to the normal drawing step. As a framework for examination of this effect, a tentative mathematical treatment was proposed based on a concept of plastic flow similar to that used to explain the response of metals in successive drawings. In this view, the spin orientation acquired during fiber formation is characterized by an effective draw ratio, $\mathcal{R}_s$. This ratio multiplied by the actual orientation draw ratio, $\mathcal{R}$, gives the total draw ratio, $\mathcal{R}_t$, for the entire process.

The purpose of the present paper is to elaborate further on the effects of spin orientation on the stress required for orientation drawing, to offer further verification of the earlier treatment, and to demonstrate its usefulness. In particular, it will be of interest to calculate actual values for the defined parameter $\mathcal{R}_s$ and

* Permanent address: Department of Chemical Engineering, The University of Texas at Austin, Austin, Texas 78712.

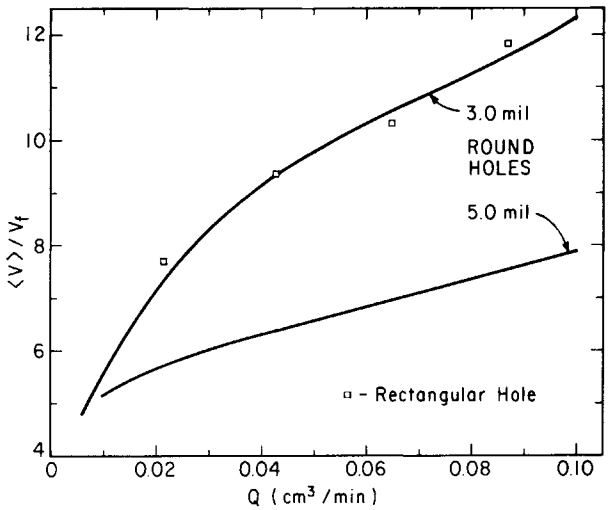

Fig. 1. Free velocity, V_f, data for acrylic spinning solutions: $\langle V \rangle$ = average dope velocity in spinneret hole.

show how it may be correlated with the rheology of fiber formation in the spin bath. Since both round and rectangular spinneret holes were used, observations on factors influencing filament shape will also be made.

EXPERIMENTAL

The details of the spinning process used in this work were given in the previous paper;[1] however, a review of some pertinent features will be useful. A spinning solution composed of an acrylic polymer dissolved in dimethylacetamide (DMAc) was pumped to a multihole spinneret at a rate of Q cm^3/min per hole. The spinneret was immersed in an aqueous spin bath containing 55% DMAc and controlled at a temperature of 55°C. The fibers were removed from the bath by a wash godet with a peripheral speed of V_1 ft/min. Next, the fibers were pulled through a boiling water orientation draw bath by a second godet with a peripheral speed of V_2. This step imparts a draw ratio $\mathcal{R} = V_2/V_1$ to the fiber. The fiber is then normally collapsed and dried, but these steps after the orientation draw are not involved in this study.

Two polymers were used in this study to establish the general applicability of the drawing model. One was the acrylic composition of the previous paper[1] and other earlier work[2-6] from this laboratory. The new polymer added was a modacrylic with a substantially different composition.

Spinneret holes with two shapes were employed here. One was the usual round hole with diameters D of 3.0, 4.5, 5.0, and 6.0 mils. The second hole shape was a rectangular slot with dimensions $H = 1.18$ and $W = 12$ mils. The rectangular hole was included because it offers a different combination of hole perimeter, hole area, and shear rate than can be obtained with round holes. This difference has important implications in the rheology of fiber formation as will be discussed in the last section of this paper.

As described previously,[4] the elastic nature of the spinning solution produces a considerable jet swell, or Barus effect, so that the fiber which emerges from the

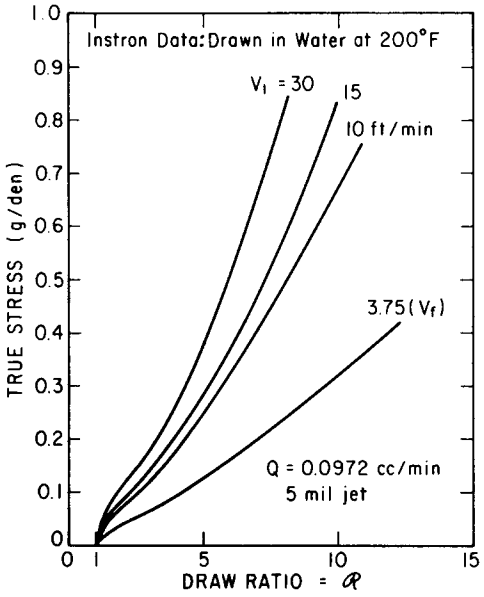

Fig. 2. Instron stress–strain curves for undrawn acrylic fibers prepared at varying take-up speeds.

hole freely (no take-up) has a velocity V_f which is significantly less than the average dope velocity in the hole $\langle V \rangle$. This free velocity has been shown earlier[4-6] to be a very useful parameter in elucidating the rheology of fiber formation and will be used again in this paper. A summary of previous V_f data for two hole sizes is plotted in Figure 1.

Two types of draw stress measurements are reported in this paper. For one, an in-line tensiometer was installed after the boiling water draw bath between godets 1 and 2 and tensions measured continuously on the moving bundle of filaments. For the second, fiber was collected after the first wash roll, kept wet, and subsequently drawn by an Instron tensile tester while immersed in water at 200°F. In both cases, the draw stress was calculated based on the instantaneous denier of the fiber after drawing; therefore, the values shown are a "true" stress rather than the usual engineering stress. Correlation of the responses observed by the in-line and Instron tests were excellent, with only one discrepancy, which will be discussed later.

RESULTS AND DISCUSSION

Figure 2 shows Instron stress–strain diagrams for four acrylic fibers collected undrawn from the first godet. Dope rate and spinning conditions were identical for all four, except for the increase in first godet speed, V_1, from 3.75 to 30 fpm.

This change greatly alters the stress–strain curves as shown. Many other graphs of this type have been generated using both Instron and in-line drawing; however, these will not be included here for the sake of brevity.

A major feature of draw stress results such as those shown in Figure 2 is that a different curve exists for each set of Q, spinneret hole, and V_1 variables. Our

purpose in this paper is to provide an explanation for this fact. Factors such as polymer composition, molecular weight, coagulant composition, and coagulation temperature greatly affect draw stress as a result of their effect on fiber structure. When polymer and coagulant are kept constant, however, spin orientation emerges as the predominant influence on draw stress, and the following analysis will consider only that factor. The first objective will be to construct a formal framework that explicitly shows the effect spin orientation has in orientation drawing. This will be done in conceptual terms first; then, an empirical mathematical relation will be introduced to summarize the effects observed in as few parameters as possible. Subsequent sections will correlate these parameters and concepts with the kinematics of fiber formation in the spin bath.

Two-Stage Drawing: An Analogy for Wet Spinning

In a wet spinning process, material deformation occurs in at least two steps, i.e., the spin bath and the orientation draw bath. It is well known that the deformation of the porous gel structure in the draw bath leads to molecular orientation. The effect of the deformation in the spin bath on molecular orientation is more difficult to define. The filament emerges from the spinneret hole as a fluid and is quickly converted to a gel network by coagulation. With no takeup to remove it from the bath the filament would emerge at a velocity V_f, but normally the take-up velocity, V_1, is much higher than V_f. Most of the resulting deformation is absorbed by the fluid portion of the filament before it coagulates. Flow of a viscoelastic fluid, such as the spinning dope, can produce orientation, but relaxation rates are rapid, and therefore deformation of viscoelastic fluids is not very effective in producing orientation. Because of the rapid rate of coagulation of acrylic or modacrylic fibers in wet spinning, however, several mechanisms exist by which deformation of the forming filament can lead to permanent orientation. Such orientation achieved prior to the first godet is called "spin orientation."

Spin orientation has been recognized as an important factor in melt spinning and has also been observed in dry spinning,[7] but only recently has its occurrence in wet spinning been demonstrated.[5] It may be detected by careful x-ray examination, but the strongest proof has been found in the sonic modulus of air-dried fibers[5] and in fiber responses such as draw stress.[1]

The effect of this preorientation on subsequent orientation drawing may be best understood by analogy to two-stage drawing of the fiber where drawing conditions are the same in both stages:

$$\text{unoriented fiber } V_0 \longrightarrow V_1 \longrightarrow V_2 \text{ final fiber}$$

$$\mathcal{R}_1 = \frac{V_1}{V_0} \qquad \mathcal{R}_2 = \frac{V_2}{V_1}$$

It might be expected that such drawing could be partitioned between the two stages in a variety of ways. The stress required to achieve a certain draw ratio in the second drawing, $\mathcal{R}_2$, would depend on the draw ratio taken in the first stage, $\mathcal{R}_1$. If the drawing conditions were identical in the two stages, then the final

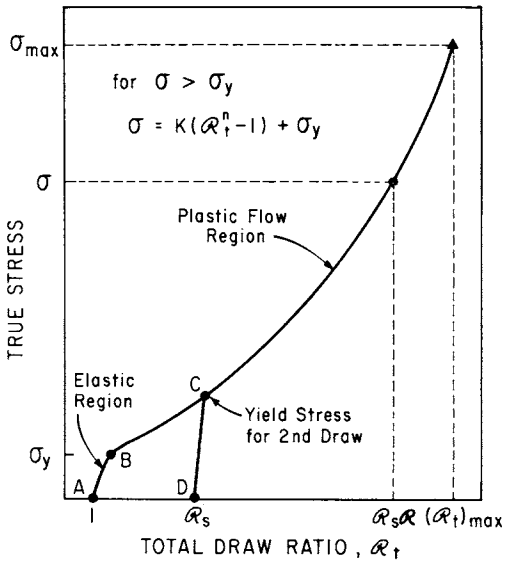

Fig. 3. Schematic stress–strain diagram for material that exhibits plastic flow.

fiber properties should be a function of the product $\mathcal{R}_1 \mathcal{R}_2$. In fact, a single draw step V_2/V_0 would produce the same effect.

We will regard the spin bath as being the first stage of a two-stage drawing operation, with the orientation draw being the second stage. The spin bath deformation is very complex, and we cannot calculate a draw ratio from the kinematics of spinning. In other words, V_0 is not known. It cannot be equated to any known velocity such as $\langle V \rangle = Q/\text{hole area}$ or V_f since the deformations involve a large component of viscous flow which produces no molecular orientation. To circumvent this problem we will assign an equivalent draw ratio to this step, designated as $\mathcal{R}_s$, and then evaluate it experimentally from the drawing behavior in the second stage. The draw ratio for the second stage will be designated simply as $\mathcal{R}$. The value $\mathcal{R}_s$ will be such that the final fiber is characterized by the product $\mathcal{R}_s\,\mathcal{R}$.

The Role of Plastic Flow

The deformation behavior of ductile solids may be divided ideally into two regions separated by the yield point of the material. Below the yield point, all deformations are elastic with nearly perfect recovery. Beyond the yield point, however, a sort of plastic flow occurs which is largely irreversible. This plastic flow is of primary interest in the drawing of fibers—a similar phenomena is also observed in many metals. There is a large body of knowledge available on the plasticity of metals which can be used by analogy to analyze fiber drawing. The following treatment will be restricted to phenomenological observations, rather than the molecular mechanisms which are undoubtedly different for polymers and metals. The methods for treating multiple drawing of metals in the plastic flow region provide a useful way to deal with spin orientation. These are described in various textbooks[8–10] and will be reviewed here.

Figure 3 shows a stress–strain diagram for a ductile material that has never

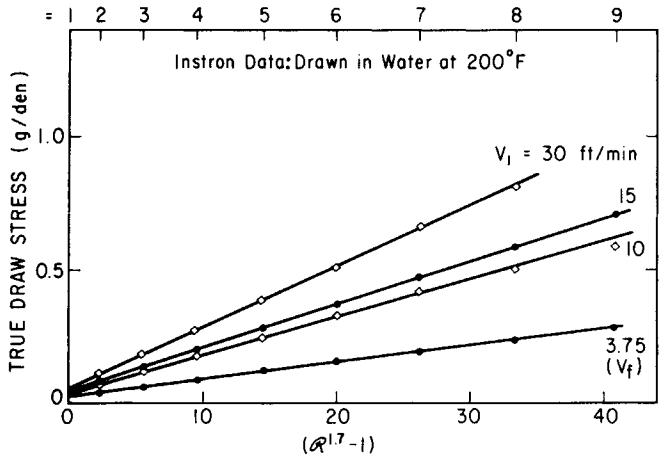

Fig. 4. Instron draw stress results on undrawn acrylic fibers plotted as suggested by eq. (2).

been drawn before and has no frozen-in stresses or orientation. The strain is expressed as a draw ratio since we will use this diagram in connection with drawing. As the material is loaded initially, it deforms along the path A to B in a purely elastic manner. Once the yield stress, σ_y, is exceeded, however, the plastic flow region is entered. There is a unique relationship between stress and strain as shown by the curve BCEX for any specified conditions of draw. There is a maximum stress or draw ratio at which failure occurs by some mechanism. A single test can be used to define the stress–strain curve BCEX. Consider now a second identical specimen which is loaded in a similar manner up to the point C and then has the stress removed. The material will elastically retract along the line CD to zero stress. When stress is reapplied, the specimen will deform again along the line DC in a purely elastic manner up to point C. Above point C, the specimen will yield and enter the plastic flow region with the relation between stress and strain following the curve CEX traced out by the first sample. It may be said that the curve BCEX is a locus of yield points.

Experience with metals has shown that once plastic flow is occurring in a second draw, then the same stress–strain relation will appear provided the deformation is referred to the original length before any extension.

Interrupted stress–strain experiments have been reported by Vincent[11] on poly(vinyl chloride) and by Rubin[12] on nylon 6. Their results on room-temperature drawing were complicated by the necking-down phenomena observed under these conditions. As a result, a yield peak was observed in the second drawing stage after partial stress relaxation, just as a yield peak occurred in the stress–strain curve for a single extension. However, when the fiber extension was interrupted in the cold-drawing region (after necking), partially relaxed, and further drawn, the stress–strain curve after passing through the small yield peak then dropped in the cold-drawing region and approximately retraced the same curve that would be obtained via a single extension. Vincent[11] found that when the load was dropped to zero after the first draw, there was no yield peak in the second extension but that the stress first increased rapidly and then continued a gradual increase to retrace the curve that would be obtained via a single extension. For the studies reported here, drawing was carried out in water at

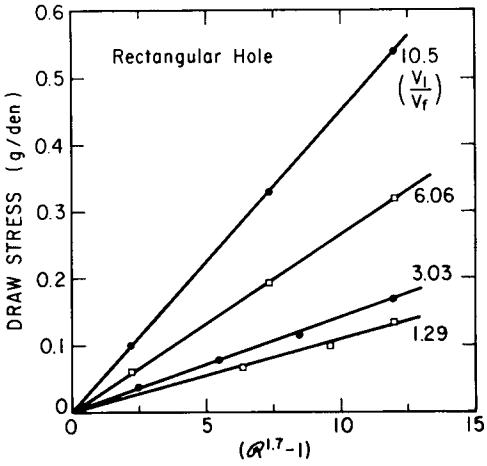

Fig. 5. In-line draw stress results on modacrylic fibers plotted as suggested by eq. (2).

200°F or higher, well above the T_g of the acrylic and modacrylic fibers. Under these conditions, no yield peak was observed in the second stage of an interrupted stretch sequence, but the stress first increased rapidly and then continued to retrace the curve obtained via a single extension.[13]

This concept may then be applied to the two-stage draw picture for the acrylic wet-spinning process. Drawing of fibers from the first godet is analogous to the second drawing described above. Different stress–strain diagrams such as those in Figure 2 are seen for each set of spinning variables because the draw stress is plotted versus the Instron draw ratio which is not calculated with reference to the true undrawn state or length. This implies that if the true undrawn length were used as a reference, there should be a single draw stress–total draw ratio curve for all four fibers in Figure 2. The observed stress σ required to draw a first godet fiber by an amount $\mathcal{R}$ either in the orientation draw bath or on the Instron is then defined by point E in Figure 3. The position of E depends on the amount of spin orientation acquired prior to the first roll which we have defined as $\mathcal{R}_s$. The larger $\mathcal{R}_s$ is, the larger will be the stress at point E in the second draw step for a given value of $\mathcal{R}$. The effective total draw ratio is given by

$$\mathcal{R}_t = \mathcal{R}_s \mathcal{R} \tag{1}$$

To pursue this picture in a quantitative fashion, a mathematical equation is needed to describe the stress–strain diagram, and the selection of such an equation is discussed next.

Selection of a Stress–Strain Equation for Plastic Flow

For the purpose of engineering stress analyses, there has been considerable effort in metals to discover suitable equations that fit the stress–strain curve in the plastic flow region. A variety of equations are available, and some have theoretical meaning. For our purposes, however, a purely empirical form is adequate, provided it fits the data. A form often used for this purpose is the following:

$$\sigma = K(\mathcal{R}_t{}^n - 1) + \sigma_y \tag{2}$$

where σ_y is the yield stress of unoriented fiber and K and n are constants. Starkweather et al.[14] have used a similar equation to describe the dependence of the yield stress on the deformation ratio for a variety of materials including many polymers. The index n appears to be a property of the material and varies widely. Equation (2) does a remarkable job of fitting all of the draw stress data presented here for both the acrylic and modacrylic fibers when the index n is assigned a value of 1.7, which was determined by statistical procedures. Equation (2) predicts that the stress to draw an unoriented filament by an amount $\mathcal{R}_s$ is

$$\sigma_s = K(\mathcal{R}_s{}^n - 1) + \sigma_y \tag{3}$$

This would be the stress at point C in Figure 3 and will become the yield stress for the second drawing. The stress to do the latter drawing, point E in Figure 3 will be

$$\begin{aligned}\sigma &= K[(\mathcal{R}_s\mathcal{R})^n - 1] + \sigma_y \\ &= K\mathcal{R}_s{}^n(\mathcal{R}^n - 1) + K(\mathcal{R}_s{}^n - 1) + \sigma_y \\ &= K\mathcal{R}_s{}^n(\mathcal{R}^n - 1) + \sigma_s\end{aligned} \tag{4}$$

From eq. (4) it is clear that if the draw stress–draw ratio relation is plotted as σ versus $(\mathcal{R}^n - 1)$, a straight line should result whose slope is $K\mathcal{R}_s{}^n$ and whose intercept is σ_s. A demonstration of the effectiveness of eq. (4) with $n = 1.7$ is given in Figure 4 using the data shown in Figure 2 for Instron drawing of the acrylic fibers. A similar demonstration is shown in Figure 5 for in-line drawing of the modacrylic polymer. All other Instron and in-line draw stress data gave equally good straight lines, which justifies the use of both the empirical eq. (2) and a common value of $n = 1.7$ for both polymers.

Close inspection of Figures 4 and 5 reveals one slight difference between the stress data measured in-line and those measured on the Instron. The Instron data in Figure 4 extrapolate to a small but finite stress at $\mathcal{R} = 1$, which increases slightly with V_1/V_f. All of the in-line stress measurements, however, extrapolate to zero stress at $\mathcal{R} = 1$, as illustrated in Figure 5. When V_1/V_f is larger than one, there should be a small relaxation stress on the fiber in the orientation draw bath even with no applied orientation draw, $\mathcal{R} = 1$. No definite reason for this observation has been established, but there are obvious differences in the mechanical arrangement and measuring device which could account for less sensitivity in the in-line measurements.

CORRELATION WITH FIBER FORMATION VARIABLES

The purpose of this section is to evaluate the parameters K and $\mathcal{R}_s$ from the experimental results and to correlate $\mathcal{R}_s$ with events in the spin bath. This will require certain assumptions and interpretations which will be presented briefly. Filaments emerge from the spinneret hole and attain a velocity V_f if no force is applied to them. This velocity is considerably less than that of the fluid in the spinneret hole, i.e, $\langle V \rangle = Q/\text{area}$ because of the recovery of the elastic deformation the fluid experienced upon entering the hole. A large body of V_f data

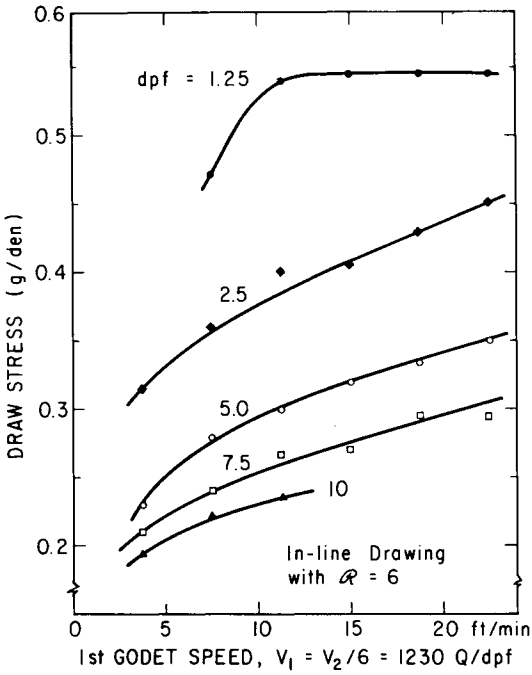

Fig. 6. In-line draw stress results on acrylic fibers with varied deniers and process speeds.

has been accumulated for the extrusion of acrylic spinning solutions through round holes.[4] A summary of such data for 3.0- and 5.0-mil-diameter holes is given in Figure 1 as a function of the dope flow rate Q. The data are plotted as $\langle V \rangle / V_f$ to emphasize the large jet swell effect.

The filaments can be removed at a higher velocity, V_1, by applying a certain force. The attenuation of filaments in this way involves a complex set of processes, and no entirely satisfactory approach has been devised to deal with its kinematics. Jet stretch, a term frequently used, has the following definition:

$$\text{jet stretch ratio} = \frac{V_1}{\langle V \rangle} \tag{5}$$

The parameter is qualitatively valid in limited comparisons but does not correlate with data from a wide range of hole sizes, hole shapes, or process speeds. This ratio in some cases is much less than one. Another ratio, V_1/V_f, has been proposed[15] which has numerous advantages over the conventional jet stretch ratio but it still does not offer a complete kinematical description of the attenuation that occurs.[6]

From an external point of view, free extrusion produces a strain-free state. Previous work[5] has shown that all freely extruded acrylic fibers have approximately the same low sonic modulus, a measure of orientation, regardless of Q or the geometry of the spinneret hole. Also no orientation was observed by x-rays. This interpretation has been successfully employed for many correlations and will be adopted in the subsequent analysis. However, it is possible to envision strains being frozen into freely extruded fibers by rapid coagulation. V_f has been shown to depend slightly on coagulation rate.[4]

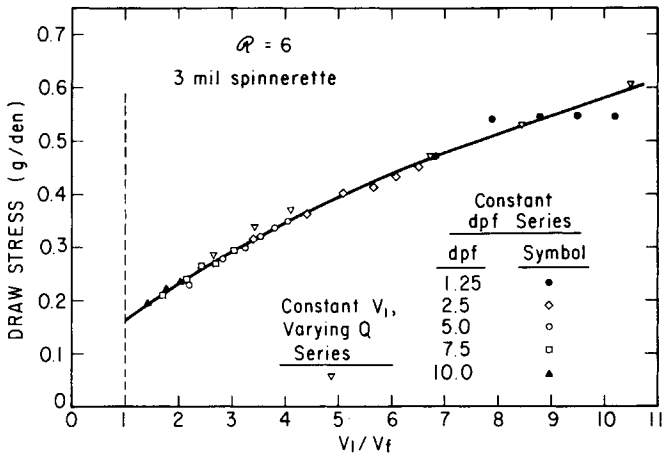

Fig. 7. Correlation of in-line draw stress data on acrylic fibers with V_1/V_f.

The ratio V_1/V_f may be regarded as the attenuation required to take the filament from the freely extruded and nearly stress-free state to its next state on the first godet, even though we recognize that the deformations involved are complex.[6] Spin orientation, as measured by sonic moduli of the undrawn fibers, has been shown to correlate better with V_1/V_f than with either jet stretch ratio, V_1/Q, or dpf.[5] In another study, it was found that the stress on the forming filament as judged by pressure reduction behind the spinneret was best correlated with the V_1/V_f ratio.[6] It was also shown that plots of pressure reduction versus $(V_1 - V_f)/V_f$ were unique for all Q, V_1, and D conditions except for small hole sizes.

The above discussion makes it reasonable to hypothesize that the effective draw ratio or orientation acquired in the spin bath, $\mathcal{R}_s$, is a function only of the V_1/V_f ratio, i.e.,

$$\mathcal{R}_s = f\left(\frac{V_1}{V_f}\right) \tag{6}$$

This hypothesis will now be tested using draw stress data obtained from the acrylic fiber. Figure 6 shows in-line data at a constant draw ratio, $\mathcal{R}$ = 6, for a series of constant denier-per-filament (dpf) fibers produced at different process speeds. To produce these fibers, Q, V_1, and V_2 were increased proportionately while using a 3.0-mil spinneret hole. The results show that the stress required for 6× orientation draw increased at higher process speeds and with smaller fiber deniers. The dpf shown is that of the final drawn fiber. Since $\mathcal{R}$ in eq. (4) is a constant for these experiments, $\mathcal{R}_s$ should be the only variable. According to the hypothesis stated in eq. (6), the observed draw stress $\sigma_{\mathcal{R}=6}$ should then be a function only of V_1/V_f. The data of Figure 6 have been replotted versus this ratio in Figure 7 where the appropriate value of V_f for each Q has been used. In addition to the data from Figure 6, results from another series of experiments in which V_1 was held constant while Q was varied are also plotted in Figure 7. All the data form a remarkable unique relationship which provides strong confirmation of the concepts developed above. In particular, the hypothesis stated in eq. (6), that $\mathcal{R}_s$ is a function only of V_1/V_f, appears valid for cases where only Q and the godet speeds are varied.

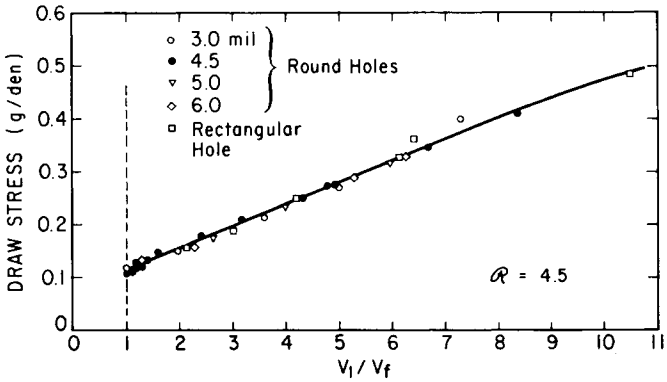

Fig. 8. Correlation of in-line draw stress data on modacrylic fibers with V_1/V_f.

Similar in-line draw stress results were obtained with the modacrylic fiber and are plotted in Figure 8. Here, the orientation draw ratio was held constant at $\mathcal{R} = 4.5$. In addition to wide variations in both Q and V_1, both the size and the shape of the spinneret hole were also varied as shown in the key to Figure 8. Again, a single unique relation is obtained when the draw stress data are plotted versus V_1/V_f. This indicates that the ideas and hypothesis outlined above are valid for the modacrylic fiber. For this fiber, the draw stress is a function of V_1/V_f also for different spinneret hole sizes and shapes. For the acrylic fibers, the relationship was valid only for fibers spun from a given hole size. Apparently, in the acylic fiber, draw stress is affected by other, as yet undefined, factors.

The data in Figures 7 and 8 are specific to the particular orientation draw ratio involved. A scheme which could fit data from various draw ratios on one plot would be useful. Such a scheme can be developed from the data collected at a range of $\mathcal{R}$ values on fibers spun under a given set of spin bath conditions. If these are plotted as shown in Figures 4 and 5, the slopes of the straight lines which result are related to $\mathcal{R}_s$ as seen by differentiating eq. (4):

$$\frac{d\sigma}{d(\mathcal{R}^{1.7} - 1)} = K\mathcal{R}_s{}^{1.7} \tag{7}$$

Since $\mathcal{R}_s$ is a function of V_1/V_f these slopes should be also. Slopes were calculated from the draw stress results on numerous modacrylic fibers. These slopes are plotted versus V_1/V_f in Figure 9. Again a remarkable unique relation is seen.

ESTIMATION OF SPIN ORIENTATION

In the previous section, we showed that the experimental data are consistent with the hypothesis that the effective draw ratio for spin orientation is uniquely determined by V_1/V_f. It would be interesting to know the absolute values of $\mathcal{R}_s$, and these can be determined by a logical extension of the discussion given earlier. Here, we hypothesize that $\mathcal{R}_s = 1$ for freely extruded filaments, i.e., when $V_1/V_f = 1$. This means that the parameter $K\mathcal{R}_s{}^{1.7}$ as shown, for example, in Figure 9 is equal to K in the limit $V_1/V_f = 1$. In this way, we can determine K and thus compute $\mathcal{R}_s$ from such results.

These calculations were made for the modacrylic fiber data in Figure 9, and

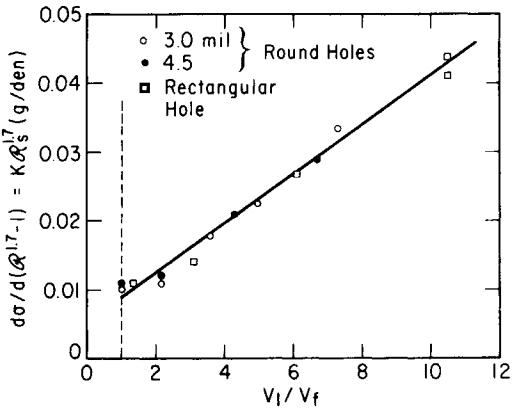

Fig. 9. Test of the hypothesis that spin bath orientation $\mathcal{R}_s$ is a function of the V_1/V_f ratio.

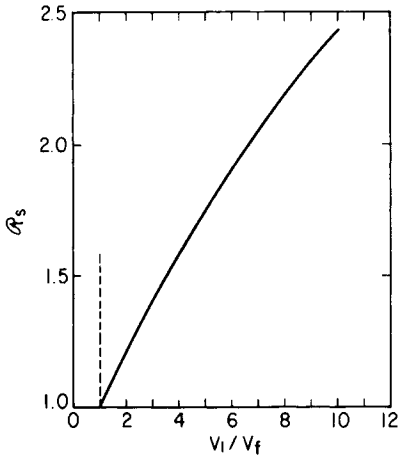

Fig. 10. Calculated spin bath orientation ratio $\mathcal{R}_s$ as a function of V_1/V_f.

the resulting $\mathcal{R}_s$ values are plotted in Figure 10 as a function of V_1/V_f. The magnitude of the $\mathcal{R}_s$ values shown in Figure 10 are reasonable, ranging from 1 to 2.4×. Thus, the maximum spin orientation developed is equivalent to drawing the same fiber 2.4× in the orientation draw bath. Although the actual value of spin orientation may be small, its effect on subsequent drawing steps can be large since the total effective draw is obtained from the product $\mathcal{R}_s\mathcal{R}$. The $\mathcal{R}_s$ values calculated for the acrylic fiber fall in the same range of 1–2.5×.

EFFECTS OF SPINNERET HOLE SHAPE

Round spinneret holes are normally used in wet spinning because they are easier to fabricate and a round filament shape is satisfactory. Noncircular holes are used to produce special filament shapes which provide desirable optical effects or other aesthetic properties. Both round and rectangular holes were employed in this study. For the round holes, dope velocity in the hole and apparent shear rate at the wall were calculated as follows:

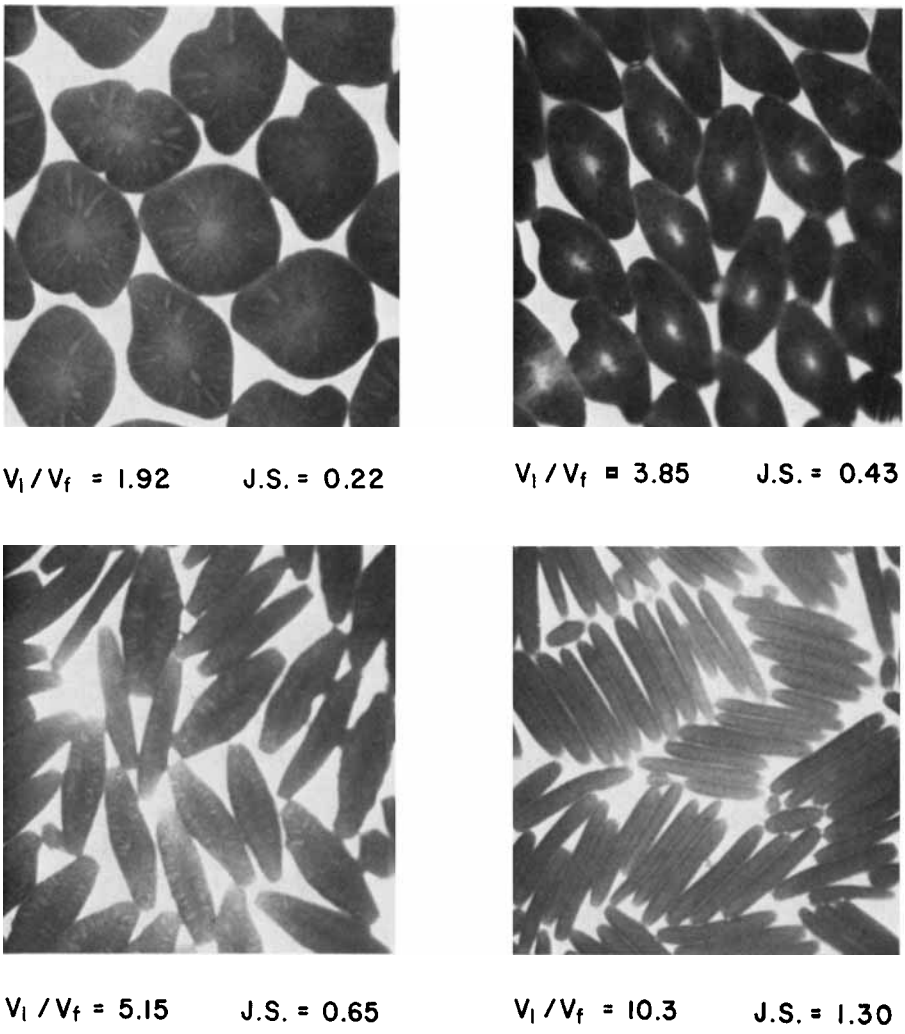

Fig. 11. Effect of V_1/V_f ratio on the shape of acrylic fibers spun from a rectangular hole with an aspect ratio of 9.8.

$$\langle V \rangle = \frac{Q}{(\pi/4)\, D^2} \qquad \text{and} \qquad \dot{\gamma}_{wa} = \frac{32Q}{\pi D^3}$$

The rectangular hole was a slot with a W/H or aspect ratio of 9.83. The average velocity through such holes and the apparent shear rate are given by the following formulas:

$$\langle V \rangle = \frac{Q}{WH} \qquad \text{and} \qquad \dot{\gamma}_{wa} = \frac{6Q}{WH^2}$$

The latter equation for shear rate is derived[16] from the approximation $W \gg H$.

The rectangular hole was of special interest in this study because it offered a different combination of hole perimeter, area, and shear rate than could be obtained with series of round hole sizes. For example, the slot hole with di-

mensions of W = 12 mils and H = 1.18 mils has the same perimeter as an 8.4-mil-diameter round hole, but its hole area is close to that of a 4.5-mil round hole. Similarly, at a given flow rate Q, the slot hole produces about the same velocity of spinning solution, $\langle V \rangle$, as the 4.5-mil round hole, but gives an apparent shear rate nearly equal to a 3.0-mil round hole. Free velocities were determined as a function of Q for the rectangular hole and are plotted in Figure 1. These show that the $\langle V \rangle / V_f$ ratio or jet swell is virtually the same as that for the 3.0-mil round hole. Since these two holes give approximately the same shear rate, it appears that shear rate controls jet swell. This is not unexpected, since earlier work found that the die swell correlated uniquely with shear rate for round holes over a range of diameters.[4]

Another interesting observation with noncircular spinneret holes is the variation obtained in filament shape. A large number of phenomena might be expected to play a role in determining the shape of wet-spun fibers. For example, even fibers spun from circular holes may be greatly distorted owing to the relative rates of solvent diffusion out, coagulant diffusion in, the rate of polymer solidification, and skin-core effects. As Han[17] has pointed out, both interfacial tension forces and normal stresses arising from extrusion will act to prevent a fiber from retaining its shape when extruded from a nonround hole. Figure 11 shows cross sections of acrylic fibers extruded through the rectangular hole used in this study and taken up at various V_1/V_f ratios as indicated. Under free extrusion conditions, one could not tell from the fiber shapes that they were extruded from a slot with an aspect ratio of nearly 10. Even at V_1/V_f = 1.92, the effect of the hole shape is barely evident. As the V_1/V_f ratio is increased, however, the shape of the fiber approaches the hole shape.

At V_1/V_f = 10.3, the aspect ratio of the fibers is nearly that of the hole, with no bulges in the middle of the sides but some rounding at the corners. Calculated jet stretch values for these samples are also shown in Figure 11. Shape retention improves as jet stretch increases from 0.22 to 1.3. Han[18] has reported that the shape of fibers spun from a noncircular hole is primarily affected by jet stretch.

CONCLUSIONS

The previous study[1] demonstrated that spin orientation was an important factor in the subsequent drawing of wet-spun acrylic fibers. It has now been established that wet spinning of both acrylic and modacrylic fibers can be treated as a two-stage drawing process, where the total orientation draw $\mathcal{R}_t$ is the product of the effective spin bath orientation $\mathcal{R}_s$ and the usual orientation draw $\mathcal{R}$. The validity of the equation proposed earlier for draw stress was confirmed for both fiber types, and it also correctly described results on fibers spun from a range of round spinneret hole sizes and a rectangular slot hole. From this equation, absolute values for the effective spin bath draw ratio $\mathcal{R}_s$ were calculated. Spin bath orientation in both fibers was shown to be a unique function of the V_1/V_f ratio for a given spinneret hole. In the modacrylic fiber, the V_1/V_f ratio also correlated with spin orientation for all spinneret hole sizes and shapes. Shape retention of fibers from the rectangular hole improved as the V_1/V_f ratio increased. These results demonstrated the validity and usefulness of the free velocity concept and V_1/V_f ratio in characterizing the effects of spin bath kinematics on fiber properties.

The authors wish to express their appreciation to Monsanto Textiles Company for permission to publish this work and to Dr. P. H. Hobson for his support and encouragement.

References

1. A. L. McPeters and D. R. Paul, *Appl. Polym. Symp.*, **25,** 159 (1974).
2. D. R. Paul, *J. Appl. Polym. Sci.*, **11,** 439 and 1719 (1967).
3. D. R. Paul, *J. Appl. Polym. Sci.*, **12,** 383 (1968).
4. D. R. Paul, *J. Appl. Polym. Sci.*, **12,** 2273 (1968).
5. D. R. Paul, *J. Appl. Polym. Sci.*, **13,** 817 (1969).
6. D. R. Paul and A. A. Armstrong, *J. Appl. Polym. Sci.*, **17,** 1269 (1973).
7. N. Teranishi, H. Iwata, and M. Hirashima, Canad. Pat. 908,377 assigned to Mitsubishi Rayon (August 29, 1972).
8. F. Seitz, *The Physics of Metals,* McGraw-Hill, New York, 1943, Chap. 6.
9. W. Johnson and P. B. Mellor, *Plasticity for Mechanical Engineers,* Van Nostrand, Englewood, N.J., 1962, Chap. 1.
10. J. N. Goodier and P. G. Hodge, *Elasticity and Plasticity,* Wiley, New York, 1958.
11. P. I. Vincent, *Polymer,* **1,** 7 (1960).
12. J. Rubin, *J. Appl. Polym. Sci.*, **16,** 1573 (1972).
13. A. L. McPeters, unpublished work.
14. H. W. Starkweather, T. F. Jordan, and G. B. Dunnington, *Polym. Eng. Sci.*, **14,** 678 (1974).
15. W. E. Fitzgerald and J. P. Craig, *Appl. Polym. Symp.*, **6,** 67 (1967).
16. J. M. McKelvey, *Polymer Processing,* Wiley, New York, 1962.
17. C. D. Han, *J. Appl. Polym. Sci.*, **15,** 1091 (1971).
18. C. D. Han and J. Y. Park, *J. Appl. Polym. Sci.*, **17,** 187 (1973).

Received January 5, 1976
Revised May 27, 1976